

## GREEN OPEN ACCESS

This is the self archived peer reviewed version of the following article:

Trudel E and Bourque CW (2010) Central clock excites vasopressin neurons by waking osmosensory afferents during late sleep. *Nature Neuroscience* 13, 467-474, which has been published in final form at

<https://www.nature.com/articles/nn.2503>

This article may be used for non-commercial purposes in accordance with Nature portfolio terms and conditions for use of self-archived versions

<https://www.nature.com/nature-portfolio/editorial-policies/self-archiving-and-license-to-publish>

## CENTRAL CLOCK EXCITES VASOPRESSIN NEURONS BY WAKING OSMOSENSORY AFFERENTS DURING LATE SLEEP

Eric Trudel and Charles W. Bourque<sup>§</sup>

Centre for Research in Neuroscience, Research Institute of the McGill University Health Center, 1650 Cedar Avenue, Montreal, QC, Canada, H3G 1A4. <sup>§</sup>to whom all correspondence should be addressed at [charles.bourque@mcgill.ca](mailto:charles.bourque@mcgill.ca).

**Osmoregulated vasopressin release is facilitated during the late sleep period (LSP) to prevent dehydration and enuresis. Previous work has shown that clock neurons in the suprachiasmatic nucleus (SCN) display low firing rates during the LSP. But it is not known how this reduced activity enhances vasopressin release. Here, we show that synaptic excitation of rat supraoptic nucleus neurons by osmosensory afferents is facilitated during the LSP. Stimulation of the SCN at this time inhibited excitatory synaptic currents induced in supraoptic neurons by activation of osmosensory afferents. This effect was associated with an increased rate of synaptic failures and occurred without changes in frequency facilitation, quantal size, or in the ratio of postsynaptic responses mediated by AMPA and NMDA receptors. We conclude that clock neurons mediate an activity-dependent presynaptic silencing of osmosensory afferent synapses onto vasopressin neurons, and that osmoregulatory gain is enhanced by removal of this effect during late sleep.**

The release of vasopressin (antidiuretic hormone) from the neurohypophysis is triggered by the electrical activity of magnocellular neurosecretory cells (MNCs) in the supraoptic (SON) and paraventricular nuclei (PVN) of the hypothalamus <sup>1</sup>. During dehydration the electrical activity of MNCs is enhanced, such that a proportional relation exists between plasma osmolality and vasopressin concentration <sup>2</sup>. This osmotic control of vasopressin release plays a key role in systemic osmoregulation because it promotes water reabsorption by the kidney in proportion with extracellular fluid osmolality <sup>2,3</sup>. It is well established that vasopressin release increases during sleep in mammals <sup>4</sup>. This phenomenon is important because it blunts the rise in plasma osmolality caused by evaporative water loss at a time when water intake is suppressed. Individuals who fail to display this circadian rhythm experience nocturnal polyuria and enuresis <sup>5</sup>. Studies in rats <sup>6</sup>, dogs <sup>7</sup> and man <sup>8</sup>, have shown that the relation between plasma vasopressin and osmolality is steepened during the late sleep period (LSP) compared with the middle of the

sleep period (MSP). Although this enhancement of osmoregulatory gain contributes to the rise in vasopressin levels during the LSP, the central basis for this effect is unknown.

The osmotic control of MNCs is mediated largely by glutamatergic afferents arising from osmosensory neurons in the organum vasculosum lamina terminalis (OVLT)<sup>2,9</sup>. Neurons in the OVLT are intrinsically osmosensitive and increase their firing rate during hyperosmolality<sup>10,11</sup>. Consequently, MNCs receive an increased rate of spontaneous excitatory postsynaptic potentials which contributes significantly to their excitation under these conditions<sup>9,12</sup>. A facilitation of this excitatory signaling between OVLT neurons and MNCs could therefore underlie the increase in central osmoregulatory gain observed during the LSP.

Previous studies have shown that the suprachiasmatic nucleus (SCN) serves as the brain's biological clock and represents a key element for the central generation of circadian rhythms<sup>13,14</sup>. Neurons in the SCN send axonal projections toward the SON<sup>12</sup> (see also Supplementary Figs. 1-3), providing a possible anatomical substrate for the circadian modulation of osmosensory signaling in this nucleus. Moreover, electrophysiological studies in nocturnal rodents have shown that SCN neurons display peak action potential firing rates during the middle of the light period (i.e. during the MSP) and minimal firing rates during the dark (i.e. wake) period<sup>15</sup>. Thus the enhancement of osmoregulatory gain during the MSP-LSP transition occurs in concert with a progressive decline in the firing rate of SCN neurons<sup>16</sup>. In this study, we therefore examined if the increase in osmoregulatory gain observed during this transition could be mediated via the disinhibition of excitatory synapses between osmosensory OVLT neurons and MNCs in the SON.

## Results

### *Osmoregulatory gain is enhanced during the LSP*

To determine if excitatory signaling between osmoreceptors and vasopressin neurons is greater during the subjective LSP than during MSP, we compared the effects of applying a local hyperosmotic stimulus to the OVLT in the presence of bicuculline (5  $\mu$ M) while recording from MNCs in slices of rat hypothalamus that preserve functional connections between the OVLT, SON and SCN<sup>12</sup> (see Supplementary Figure 1). Local hyperosmotic stimulation of the OVLT significantly increased the action potential firing rate of MNCs during both the MSP and the LSP (**Fig. 1a,b**). The excitation of MNCs in these experiments was not associated with a significant change in baseline membrane potential ( $P = 0.195$ ,  $n = 9$  in MSP and  $P = 0.275$ ,  $n = 9$  in LSP), indicating that the response was mediated by osmosensory afferents and not by other osmosensory mechanisms present in the SON<sup>2</sup>. Indeed, local hyperosmotic stimulation of the OVLT significantly increased the frequency of spontaneous excitatory postsynaptic currents (sEPSC; **Fig. 1c**) recorded in voltage-clamped MNCs during both the MSP (control  $1.1 \pm 0.2$  Hz vs hyperosmotic  $1.4 \pm 0.3$  Hz ;  $n = 14$  ;  $P < 0.001$ ) and the LSP (control  $2.7 \pm 0.7$  Hz vs hyperosmotic  $4.4 \pm 0.8$  Hz ;  $n = 10$  ;  $P = 0.0036$ ). The average effects of osmotic stimulation on action potential firing rate and sEPSC frequency were both significantly greater when evoked during the LSP than during the MSP (**Fig. 1d**). The frequency of action potentials and sEPSCs respectively increased by  $22.2 \pm 6.9$  % and  $36.2 \pm 8.7$  % during the MSP, compared to  $115.9 \pm 39.9$  % ( $P = 0.03$ ) and  $95.7 \pm 27.7$  % ( $P = 0.03$ ) during the LSP (values are means and s.e.m. of the average percent changes observed in each cell). Control experiments (see Supplementary Figure 4) confirmed the existence of a progressive increase in osmoregulatory gain during the transition from the MSP to the LSP, and showed that the age of the slice (amount of time after surgical preparation) was not a determining factor in our experiments. Thus the transfer of

synaptic information between osmoreceptors and MNCs is significantly enhanced during the MSP-LSP transition.

### *Clock neurons inhibit osmosensory afferents*

To confirm that SCN neurons maintain their circadian rhythmicity in the horizontal slice preparation, extracellular recordings of spontaneous action potential firing were obtained from SCN neurons during the MSP and LSP (e.g. **Fig. 2a**). The mean ( $\pm$  s.e.m.) firing rate of these cells was significantly slower when recorded during the LSP ( $1.6 \pm 0.3$  Hz ;  $n = 20$ ) than during the MSP ( $3.8 \pm 0.7$  Hz ;  $n = 16$  ;  $P = 0.0035$ ; **Fig. 2b,c**). Since osmosensory signaling is weaker when the firing rate of SCN neurons is high (i.e. during the MSP), we hypothesized that SCN neurons actively inhibit glutamatergic synaptic transmission between OVLT neurons and MNCs (i.e. OVLT-MNC synapses). To test this hypothesis, we examined the effects of repetitive electrical stimulation of the SCN on the amplitude of EPSCs evoked by low frequency (0.1 Hz) electrical stimulation of the OVLT. Stimulation of the SCN at 5 Hz caused a rapid, sustained and reversible inhibition of EPSC amplitude (**Fig. 3a,b**). Indeed, no adaptation was observed during stimulation trials lasting up to 15 min (data not shown). Data collected from 116 MNCs revealed that the inhibition of OVLT-MNC synapses increases as a function of stimulation rate between 0.1 Hz and 20 Hz, with a half maximal effect occurring at 3.0 Hz (**Fig. 3c**). The spontaneous action potential firing rates observed in SCN neurons during the MSP and LSP (**Fig. 2**) could therefore mediate significantly different degrees of inhibition on OVLT-MNC synapses.

To confirm that the effects of electrical stimulation of the SCN were not simply due to the activation of fibers of passage, we also examined the effects of selectively exciting SCN

neurons by local application of glutamate on EPSCs evoked in MNCs by electrical stimulation of the OVLT (**Fig. 4a**). As illustrated in **Fig. 4b**, the amplitude of EPSCs evoked by OVLT stimulation was reversibly reduced when glutamate was applied over the SCN. The average effects of glutamate application measured in 6 cells are shown in **Fig. 4c**. In these experiments the average amplitude of EPSCs evoked under control conditions ( $-39.6 \pm 11.4$  pA) was significantly reduced when measured during the last 30 s of the glutamate application to the SCN ( $-22.2 \pm 5.8$  pA;  $n = 6$ ;  $P < 0.05$ ).

#### *Vasopressin mediates part of the clock's inhibitory effect*

The inhibitory effect of the SCN on OVLT-MNC synapses is presumably caused by the activity-dependent release of a neuromodulator substance. The possible involvement of  $\gamma$ -amino butyric acid (GABA) type A ( $\text{GABA}_A$ ) receptors was already excluded by the fact that all of the experiments reported above were performed in the presence of bicuculline. We therefore examined the possible role of metabotropic receptors recognizing glutamate, GABA, adenosine and vasopressin. These substances are contained in SCN neurons<sup>17-19</sup> and have been shown to inhibit excitatory transmission in the SON<sup>20-23</sup>. The inhibitory effects of SCN stimulation on OVLT-MNC synapses tested during the LSP were not affected by bath application of MAP-4 (25  $\mu\text{M}$ ;  $n = 6$ ;  $P = 0.851$ ; antagonist of Group III metabotropic glutamate receptors), SCH50911 (3  $\mu\text{M}$ ;  $n = 9$ ;  $P = 0.547$ ; antagonist of  $\text{GABA}_B$  receptors), or DPCPX (2  $\mu\text{M}$ ;  $n = 16$ ;  $P = 0.525$ ; antagonist of A1 adenosine receptors). However bath application of 2  $\mu\text{M}$  Manning compound, a broad spectrum inhibitor of vasopressin receptors<sup>23</sup>, significantly reduced the effect of SCN stimulation. Indeed, the percent inhibition of EPSCs induced by

sustained stimulation of the SCN at 5 Hz was reduced from  $54.7 \pm 5.3$  % in control to  $36.7 \pm 7.5$  % in the presence of Manning compound ( $P = 0.0125$  ;  $n = 8$  ; see Supplementary Figure 5).

To determine if vasopressin receptors specifically contribute to the inhibition of osmosensory signaling during the MSP, we examined the effects of Manning compound on the increase in sEPSC frequency induced in MNCs by hyperosmotic stimulation of the OVLT. Data obtained in 4 MNCs showed that the osmotically induced increase in sEPSC frequency observed at this time was significantly greater in the presence of Manning compound ( $+0.29 \pm 0.06$  Hz) than under control conditions ( $+0.07 \pm 0.06$  Hz ;  $P < 0.05$ ; paired t-test). The inhibitory effect of the SCN on OVLT-MNC synapses is thus mediated in part via the activation of vasopressin receptors.

#### *Excitation of clock neurons impairs osmosensory signaling*

To determine if the activity-dependent inhibition of OVLT-MNC synapses mediated by the SCN can functionally impair osmosensory signaling, we next examined if the excitation of SCN neurons by glutamate could attenuate the effect of local hyperosmotic stimulation of the OVLT on MNCs recorded during the LSP (**Fig. 5a**). As illustrated in **Fig. 5b**, the osmotic excitation of MNCs was inhibited during application of glutamate to the SCN. Similarly, the osmotically-induced increase in sEPSC frequency was smaller when glutamate was being applied to the SCN (**Fig. 5c**).

Globally, there was a statistically significant reduction in osmotically-induced changes in both action potential firing rate ( $107.1 \pm 11.7$  % during SCN glutamate compared with  $191.9 \pm 35.1$  % without;  $n = 11$  ;  $P = 0.026$ ) and sEPSC frequency ( $98.6 \pm 4.8$  % during SCN glutamate compared with  $178.6 \pm 29.7$  % without ;  $n = 9$  ;  $P = 0.046$ ) when SCN neurons were

being excited by locally-applied glutamate (**Fig. 5d**). Raising the electrical activity of SCN neurons can therefore functionally inhibit the transfer of osmosensory information between OVLT neurons and MNCs.

#### *Osmosensory afferents are inhibited presynaptically*

We next investigated the mechanism underlying the SCN-mediated inhibition of OVLT-MNC synapses. Previous studies have shown that decreases in EPSC amplitude can be caused by the modulation, or endocytosis, of postsynaptic AMPA ( $\alpha$ -amino-3-hydroxy-5-methyl-4-isoxazole propionic acid-type) receptors (AMPA receptors) <sup>24, 25</sup>. Inhibition of AMPARs under these conditions typically occurs in the absence of a change in the response evoked by N-methyl-D-aspartate receptors (NMDARs) expressed at the same synapses. However as illustrated in **Fig. 6a**, the amplitude of NMDAR responses (measured at +40 mV) varied in concert with that of AMPAR responses during the dynamic (i.e. onset and offset) periods of SCN stimulation (**Fig. 6b**). Moreover, the average ratio of absolute response amplitudes mediated by each receptor subtype (the AMPAR:NMDAR ratio) was not significantly different when measured before ( $0.90 \pm 0.14$ ) or during steady-state SCN-mediated inhibition ( $0.79 \pm 0.12$ ;  $n = 8$ ;  $P = 0.1917$ ; not shown).

A recent study has shown that electrically-evoked EPSCs recorded in MNCs are followed by a transient increase in the probability that single glutamate vesicles are released at the stimulated synapses in MNCs <sup>26</sup>. To determine if unitary (quantal) amplitude at OVLT-MNC synapses was affected by the activation of SCN neurons, we therefore analyzed the asynchronous EPSCs (aEPSCs) detected immediately following the synchronous EPSC evoked by electrical OVLT stimulation. Activation of SCN neurons with glutamate reduced the average

frequency of aEPSCs from  $28.6 \pm 9.0$  Hz in control to  $20.5 \pm 6.5$  Hz ( $n = 6$  ;  $P < 0.05$ ; e.g. **Fig. 6c**). However the amplitude of these events was not changed during SCN stimulation (control  $-35.9 \pm 3.3$  pA vs SCN  $-29.0 \pm 1.7$  pA ;  $P > 0.05$  ; **Fig. 6d,e**). We also examined the effects of repetitive electrical stimulation of the SCN at 5Hz on aEPSCs. As observed with glutamate application, this procedure had no effect on the amplitude of aEPSCs but caused a significant reduction in the frequency of these events ( $P = 0.001$ ;  $n = 11$ , data not shown). Taken together, these results indicate that postsynaptic AMPARs are not affected by SCN stimulation, suggesting that the inhibition of OVLT-MNC synapses is mediated at a presynaptic level.

#### *Clock neurons promote presynaptic silence*

Presynaptic inhibition can be caused by a decrease in the probability of transmitter release ( $P_r$ ) induced by reducing the voltage-gated  $Ca^{2+}$  influx associated with the arrival of an action potential into the presynaptic terminal, or by uncoupling  $Ca^{2+}$  influx and exocytosis<sup>25</sup>. In either case, the reduced coupling between APs and exocytosis increases the number of instances where presynaptic impulses fails to trigger vesicle fusion (i.e. cause synaptic failures). As illustrated in **Fig. 7a**, SCN-mediated inhibition of OVLT-MNC synapses was associated with an increase in the rate of synaptic failures. Specifically, dynamic changes in the rate of synaptic failures monitored during the onset and offset of SCN-mediated inhibition were positively correlated with the corresponding strength of the inhibitory effect (slope  $0.17 \pm 0.02$  ;  $r^2 = 0.577$  ;  $n = 63$  ;  $P < 0.0001$  ; **Fig. 7b**). Moreover, the average rate of failures monitored during the steady-state phase of SCN stimulation ( $13.5 \pm 0.9$  %) was significantly greater than that observed under control conditions ( $0.7 \pm 0.3$  % ;  $n = 63$  ;  $P < 0.001$ ; data not shown). The

inhibitory effect of the SCN is therefore caused by a decrease in presynaptic  $P_r$  at OVLT-MNC synapses.

Presynaptic inhibition caused by a reduction in action potential mediated  $Ca^{2+}$  influx is commonly associated with an increase in frequency-dependent facilitation<sup>27</sup>. However, the degree of facilitation observed when pairs of EPSCs were evoked 50 ms apart (paired pulse ratio,  $PPR = EPSC_2/EPSC_1$ ) was not changed during SCN-mediated inhibition (**Fig. 7c**). Dynamic values of PPR monitored during the onset and offset periods of SCN-mediated inhibition were not correlated to the inhibition of the first EPSC (**Fig. 7d**; slope  $-0.004 \pm 0.003$  ;  $r^2 = 0.073$  ;  $P = 0.19$ ), and the average PPR measured during the steady-state inhibition ( $1.28 \pm 0.11$ ) was not significantly different than that observed in control ( $1.47 \pm 0.08$  ;  $n = 25$  ;  $P = 0.12$  ; data not shown). By contrast the inhibition of OVLT-MNC EPSCs caused by bath application of baclofen, which is due to a presynaptic inhibition of  $Ca^{2+}$  influx<sup>28,29</sup>, was accompanied by a significant increase in PPR (Supplementary Fig. 6). These observations indicate that SCN-mediated inhibition of OVLT-MNC synapses is caused by a decrease in  $P_r$  that is independent of  $Ca^{2+}$  influx.

If an increase in  $P_r$  caused by disinhibition of afferents is responsible for the enhancement of osmosensory signaling on MNCs, then the basal frequency of sEPSCs recorded in MNCs should be higher during the LSP than the MSP. Indeed, as illustrated in **Fig. 8a**, the basal frequency of sEPSCs measured in MNCs was significantly greater during the LSP ( $2.70 \pm 0.49$  Hz ;  $n = 19$ ) than during the MSP ( $1.74 \pm 0.17$  Hz ;  $n = 58$  ;  $P < 0.05$  ; **Fig. 8b**). If this difference reflects a tonic activity-dependent presynaptic modulation of OVLT-MNC synapses by the central clock, then changing the activity of SCN neurons should cause inversely proportional changes in the rates of sEPSCs recorded in MNCs. In agreement with this hypothesis, the frequency of sEPSCs measured during the LSP was significantly reduced by

local application of glutamate over the SCN (70.0 % relative to control ; n = 12 ; P = 0.01 ; **Fig. 8c,d**). Conversely, the basal frequency of sEPSCs measured during the MSP was significantly enhanced by local application of GABA over the SCN (138.7 % compared with control; n = 7; P = 0.002; **Fig. 8e,f**).

## Discussion

Centrally-driven circadian rhythms are regulated by the SCN, an intrinsic biological clock entrained by daylight via afferents originating in the eye<sup>14,15</sup>. Studies in rodents have shown that SCN neurons display higher action potential firing rates during sleep than during the wake period, with a notable slowing of their electrical activity during the transition from MSP to LSP<sup>15,16</sup>. This rhythm is preserved when the SCN is surgically deafferented *in vivo*<sup>30</sup>, and is maintained *in vitro* in hypothalamic slices<sup>31-33</sup> and in neurons acutely isolated from the SCN<sup>34</sup>. Recent studies have revealed that cell-autonomous transcriptional feedback loops drive changes in gene expression that may play a key role in the regulation of circadian rhythms at a cellular level<sup>14,34</sup>. However the mechanisms by which changes in the electrical activity of clock neurons impart circadian changes in the function of central networks remain unknown. The objective of our study was to define how a decrease in the firing rate of SCN neurons may facilitate the osmotic control of action potential firing in MNCs during the MSP-LSP transition. Previous electrophysiological work<sup>12</sup> and anatomical data shown in Supplementary Figures 2 and 3 suggests that SCN neurons might directly communicate with MNCs in the SON. However definitive evidence for the existence of a monosynaptic projection between the SCN and the SON remains to be obtained. Although our results show that changes in clock neuron firing frequency modulate the osmotic regulation of MNCs, it remains to be determined if this effect was mediated directly, or via peri-SON interneurons that might have relayed the information provided by clock neurons to MNCs via feed-forward connections.

### *Osmotic activation of MNCs is enhanced during late sleep*

Acute changes in extracellular fluid osmolality can cause severe neurological problems and mammals avoid these through the central orchestration of homeostatic systems that preserve

salt and water balance<sup>2</sup>. When plasma osmolality rises above the set-point during waking hours, water intake is increased through the sensation of thirst and renal water reabsorption is enhanced by the release of vasopressin. Studies in various mammals<sup>6,7</sup>, including man<sup>8</sup>, have shown that the proportional relation between osmolality and vasopressin is progressively enhanced during sleep, thereby maximizing water conservation at a time when water intake is suppressed. In rats, hyperosmotic conditions also excite oxytocin-releasing MNCs<sup>35,36</sup> and the resulting increase in circulating oxytocin has a natriuretic effect on the kidney that promotes homeostasis<sup>37-39</sup>. As found for vasopressin, the osmotic control of oxytocin release is also sensitized during late sleep<sup>4</sup>. These increases in neurohypophysial hormone release during the LSP exemplify the importance of circadian rhythms in the dynamic adaptation of homeostatic systems to changing physiological requirements during the sleep-wake cycle<sup>4,5,13,18,40</sup>.

Previous studies in rats have shown that osmosensory neurons located in the OVLT play a determinant role in the osmotic control of both vasopressin and oxytocin releasing MNCs<sup>2,41,42</sup>, and that this effect is mediated via glutamatergic synapses<sup>2,9,12</sup>. In this study we therefore specifically examined if glutamatergic signaling between OVLT neurons and MNCs could be modulated by changes in the activity of clock neurons during the MSP-LSP transition. Slightly more than half of the MNCs in the rat SON synthesize vasopressin, whereas the remainder contain oxytocin. Although we did not specifically identify the peptides contained in the cells we analyzed, all SON MNCs which we studied were similarly affected by SCN stimulation. It is therefore likely that both oxytocin and vasopressin releasing MNCs experience the same modulatory influence mediated by SCN clock neurons.

*SCN neurons inhibit osmosensory signaling*

In angled horizontal slices of rat hypothalamus that maintain functional connections between the OVLT, SON and SCN *in vitro*<sup>12</sup>, we observed that the excitation of MNCs caused by a hyperosmotic stimulus delivered to the OVLT was significantly greater during the projected LSP than during the MSP. Because vasopressin and oxytocin secretion is determined by the firing rate of MNCs<sup>1,2</sup>, this finding provides a likely explanation for the circadian enhancement of osmoregulated neurohypophysial hormone release during the LSP *in vivo*<sup>6-8</sup>. Previous work has shown that the excitation of MNCs during local hyperosmotic stimulation of the OVLT is due specifically to the activation of AMPARs at glutamatergic synapses made onto MNCs by osmosensitive OVLT neurons<sup>9,12</sup>. In agreement, we found that the excitation of MNCs under these conditions was associated with an increase in the frequency of sEPSCs. Moreover, the hypertonicity-induced increase in sEPSC frequency was greater during the LSP than during the MSP, with a measurable transition from low to high synaptic excitation during the MSP-LSP transition (Supplementary Figure 4c). Because the firing rate of SCN neurons is inversely related to this change in osmotically-induced synaptic excitation, we hypothesized that SCN neurons mediate an activity-dependent inhibition of synaptic transmission at OVLT-MNC synapses. Indeed, increasing the activity of SCN neurons with glutamate significantly reduced the increase in sEPSC frequency and action potential firing rate observed in MNCs during hyperosmotic stimulation of the OVLT (**Fig. 5**).

To determine if this effect was due specifically to an effect on synaptic strength, we examined the effects of SCN activation on excitatory transmission evoked in MNCs by direct electrical stimulation of the OVLT. We found that chemical excitation of SCN neurons with glutamate could directly inhibit the amplitude of EPSCs evoked at OVLT-MNC synapses (**Fig. 4**). Moreover electrical stimulation of the SCN caused a sustained and activity-dependent reduction in the amplitude of these EPSCs (**Fig. 3**), and the frequency-dependence of this effect spanned the range of spontaneous firing frequencies observed in SCN neurons during the MSP

(~4 Hz) and the LSP (~1.5 Hz; **Fig. 2**). These findings indicate that the higher firing rate of SCN neurons during the MSP caused a tonic inhibition of OVLT-MNC synapses and that the increase in osmoregulatory gain observed during the LSP was associated with a reversal of this effect (i.e. disinhibition).

#### *Vasopressin contributes to clock-mediated inhibition*

The identity of the neurotransmitters responsible for the activity-dependent inhibition of OVLT-MNC synapses remains to be fully established. A preliminary assessment of potential candidates revealed that vasopressin plays an important role in this process. Indeed, vasopressin is synthesized by a large subset of SCN neurons<sup>43</sup>. Moreover, exogenous vasopressin has been shown to inhibit excitatory synapses on MNCs in the SON<sup>23,44</sup>, and data shown in Supplementary Figure 5 reveals that part of the inhibitory effect of SCN stimulation on OVLT-MNC synapses was blocked by Manning compound, an inhibitor of vasopressin receptors<sup>45</sup>. This inhibitor also significantly enhanced the increase in sEPSC caused by hyperosmotic stimulation of the OVLT during the MSP, indicating that endogenous release of vasopressin mediates a tonic inhibitory effect on the synaptic activation of MNCs by osmosensory afferents during the MSP.

Previous work has shown that MNCs also release vasopressin from their dendrites in response to excitation<sup>44</sup>. We therefore considered the possibility that the inhibition of OVLT-MNC synapses was due to indirectly to vasopressin release by surrounding MNCs that might become excited during SCN stimulation. However we found that repetitive stimulation of the OVLT at 20 Hz (which excites MNCs) did not inhibit glutamatergic EPSCs evoked in MNCs by low frequency (0.1 Hz) electrical stimulation of the SCN (Supplementary Figure 7). This finding indicated that the effect of SCN stimulation on OVLT-MNC synapses is specific and

that vasopressin released by the axon terminals of SCN neurons contributed to their inhibitory influence on osmosensory afferents. Nonetheless, it must be noted that bath application of 2  $\mu$ M Manning Compound only partly blocked the inhibitory effect of SCN stimulation on OVLT-MNC synapses (Supplementary Figure 5). Whether this residual inhibitory effect is due to an incomplete blockade of vasopressin receptors, or to the involvement of another transmitter, remains to be determined.

### *Mechanisms of clock-mediated inhibition*

The increased rate of synaptic failures and the absence of changes in the ratio of AMPAR:NMDAR responses during SCN-mediated inhibition of OVLT-MNC synapses suggested that SCN neurons exert their inhibitory influence at a presynaptic locus. In agreement with this hypothesis, we found no effect of SCN stimulation on postsynaptic responses to exogenous AMPA (Supplementary Figure 8) and the inhibitory effect of SCN stimulation was not impaired by blocking postsynaptic G-protein coupled receptor signaling with GDP- $\beta$ -S (Supplementary Figure 9). Moreover, SCN stimulation had no effect on the amplitude of the aEPSCs evoked by stimulation of the OVLT, indicating that quantal size is unaffected at the synapses which are specifically inhibited by SCN stimulation. Collectively, these findings indicate that a proportion of OVLT-MNC synapses become latent as the firing rate of SCN neurons rises, and that this effect is due to a "switching off" of transmitter release at these synapses. Remarkably, SCN stimulation had no effect on the PPR, an index of frequency facilitation that is enhanced when action potential triggered  $\text{Ca}^{2+}$  influx is reduced in the presynaptic terminal<sup>27</sup>. We therefore conclude that the effects of SCN stimulation are not mediated by graded changes in presynaptic [ $\text{Ca}^{2+}$ ] dynamics, but by a reversible and  $\text{Ca}^{2+}$ -

independent suppression (i.e. silencing) of transmitter release<sup>46,47</sup>. The basis for this effect remains to be determined.

The results of our experiments indicated that the amplification of OVLT-mediated osmosensory signaling during the MSP-LSP transition is mediated in part by an increase in the number of functional synapses relaying osmosensory information from the OVLT. However previous work has also shown the existence of functional connections from the SCN to the OVLT<sup>12</sup>. It is therefore possible that changes in the firing rate of SCN neuron could also increase the responsiveness of OVLT neurons to locally applied osmotic stimuli, and thereby participate in the enhancement of osmoregulatory gain during the LSP. Additional experiments are required to explore this possibility. As noted earlier, circulating levels of vasopressin and oxytocin rise progressively throughout the sleep period and reach a peak at the end of the LSP<sup>4</sup>. This rhythm does not exactly mirror average changes in the firing rate of SCN neurons which peak during the MSP<sup>15</sup>. Although our data shows that the reduction in SCN neuron firing rate contributes to the enhancement of osmosensory signaling during the MSP-LSP transition, the mechanisms by which MNCs and neurohypophysial hormone secretion are regulated during other parts of the circadian cycle remain to be determined. Many of the other parameters that modulate MNCs also display pronounced diurnal rhythms that occur in and out of phase with neurohypophysial secretion; including changes in blood pressure, body temperature and circulating hormones such as cortisol and melatonin<sup>13,40</sup>. Additional studies are required to define how these other factors influence the circadian changes in MNC firing and neurohypophysial hormone release.

*Concluding statement.*

Previous work has shown that synaptic gain can be altered by activity-dependent long-term potentiation or depression through the respective insertion or removal of AMPARs<sup>25</sup>. These postsynaptic forms of synaptic plasticity have been shown to occur in MNCs<sup>48, 49</sup> where, as in other neurons, they can alter the relative impact of subsets of synapses that are important for the control of excitability. Interestingly, recent studies have shown that subsets of synapses can be made latent ("silenced") by an inactivation of transmitter release at the presynaptic level<sup>46, 47, 50</sup>. This mechanism potentially allows specific pathways to be temporarily removed from a neural circuit without affecting the long-term adjustments made at the post-synaptic level. Our study reveals that clock neurons in the SCN use this process to reversibly modulate the number of functional synapses between OVLN neurons and MNCs in a manner that explains the enhancement of osmoregulated vasopressin release during the late stage of sleep. Whether central clock neurons modulate other central circuits by a similar mechanism remains to be determined.

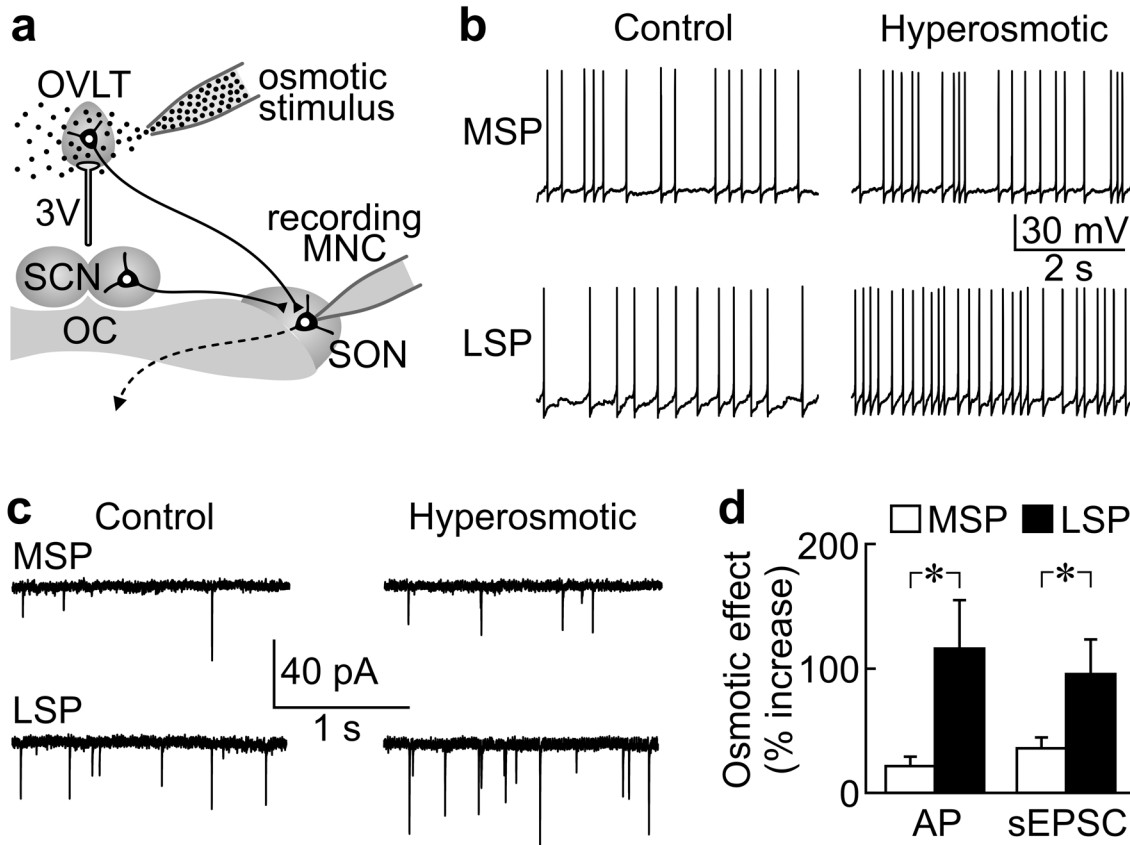
### **Acknowledgements**

This work was supported by operating grant MOP-9939 from the Canadian Institutes of Health Research (CIHR) and a James McGill Chair to C.W.B. E.T was recipient of a Doctoral Studentship from the Heart and Stroke Foundation of Canada. The Research Institute of the McGill University Health Centre is supported by the Fonds de la Recherche en Santé du Québec. The authors thank Drs. K.K. Murai and W.T. Farmer (McGill University) for help with the anterograde experiments (Supplementary Fig. 2), and Ms. Méline Henry and Dr. Didier Mougnot (Laval University) for help with the retrograde labelling experiments (Supplementary Fig. 3).

### **Author contributions**

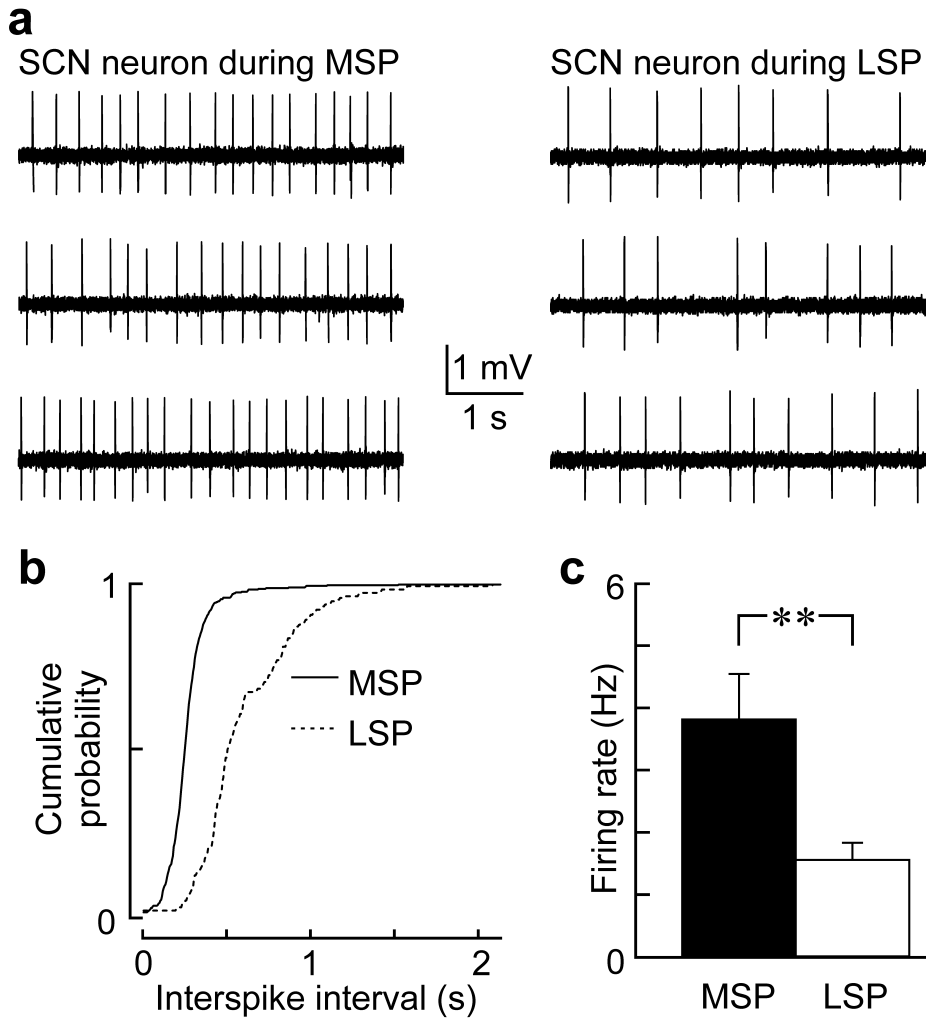
All of the electrophysiological experiments, technical development and data analysis were performed by E.T. C.W.B. designed the experimental approaches and wrote the paper in close consultation with E.T.

Figure 1



**Figure 1. Increased osmoregulatory gain during LSP.** (a), diagram showing the positions and axonal projections of the OVLT, SCN and SON relative to the third ventricle (3V) and optic chiasma (OC) in the angled horizontal slice of rat hypothalamus. Whole cell recordings were made from MNCs in the SON and hyperosmotic stimuli (excess mannitol) were delivered locally to the OVLT via a small pipette. (b), traces show examples of action potential (AP) firing recorded from an MNC before (control) and during hyperosmotic stimulation of the OVLT. The top traces are from a cell recorded during the MSP and the lower traces are from a cell during the LSP. (c), traces (arranged as in b), show examples of sEPSC activity recorded under voltage clamp ( $V_{hold} = -70$  mV). (d), bar graphs showing the mean ( $\pm$  s.e.m.) normalized osmotically-induced increases in AP and sEPSC frequency recorded from cells tested during the MSP or the LSP. \* indicates  $P < 0.05$ .

## Figure 2



**Figure 2.** Firing rate of SCN neurons during the MSP and LSP in angled horizontal slices of rat hypothalamus. (a), consecutive traces obtained during extracellular recordings of spontaneous action potential firing in representative SCN neurons recorded during the MSP (left) and LSP (right). (b), cumulative probability distributions of inter-action potential intervals recorded from the cells shown in a. The plots are constructed from 448 action potentials recorded from the MSP cell and 195 action potentials recorded from the LSP cell. (c), Bar histogram comparing the mean ( $\pm$  s.e.m.) firing rates recorded from SCN neurons sampled during the MSP ( $n = 16$ ) and LSP ( $n = 20$ ). \*\* indicates  $P < 0.005$ .

**Figure 3**

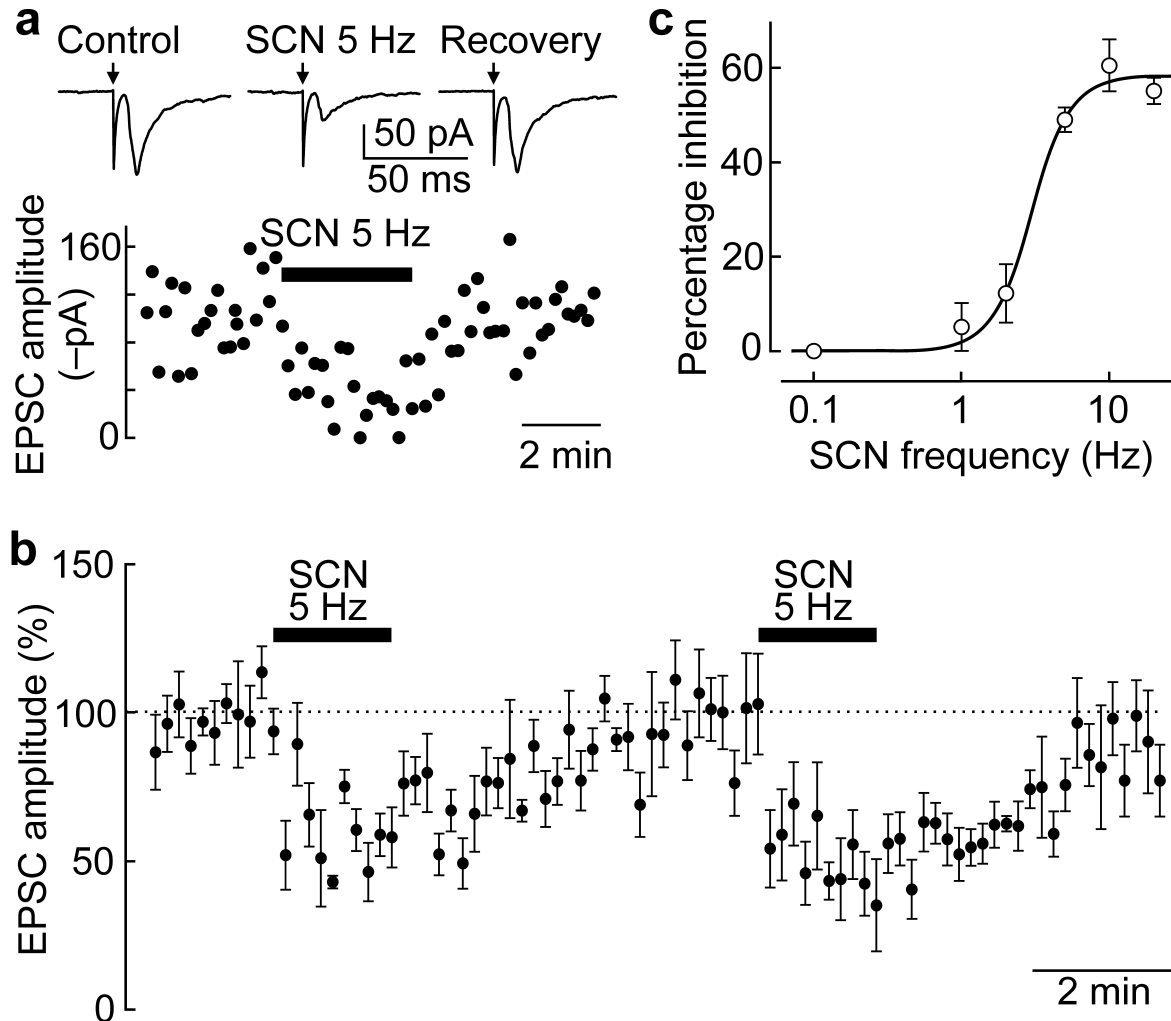


**Figure 3.** Electrical stimulation of SCN inhibits OVLT-MNC synapses. (a), upper panels show examples of EPSCs evoked in an MNC by stimulation of the OVLT (arrows; 0.1 Hz). Each trace is an average of 15 consecutive sweeps recorded before (control), during (SCN 5Hz; gray bar in lower panel), and after (recovery) continuous repetitive electrical stimulation of the SCN at 5 Hz. The lower panel is a plot of the absolute peak amplitudes of all single EPSCs recorded during this experiment. (b), plot showing the mean ( $\pm$  s.e.m.) changes in EPSC amplitude at OVLT-MNC synapses evoked by SCN stimulation at 5 Hz (gray bars) observed in 8 cells. Values are expressed as a percent of baseline (dotted line; mean of the values recorded 100 s before SCN stimulation in each cell). (c), Graph showing the mean ( $\pm$  s.e.m.) percent inhibition of the evoked OVLT-MNC EPSC induced by repetitive stimulation of the SCN at various frequencies. The solid line is a best fit through the data points using a 3 parameter logistic equation, where  $a = 57.1\%$ ,  $b = -3.84$  and  $x_0 = 3.05$  Hz ( $r^2 = 0.993$ ; see online Methods).

**Figure 4**

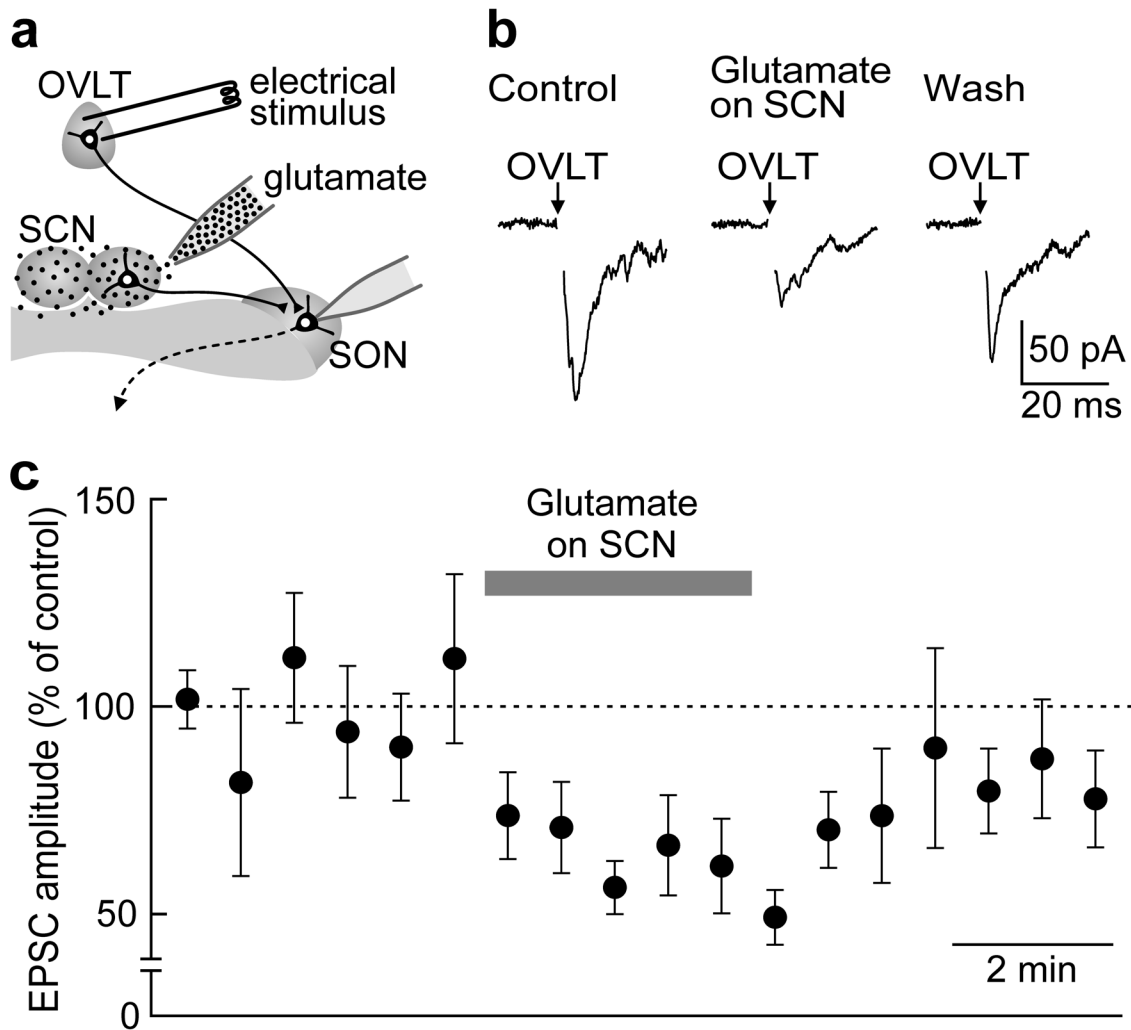


**Figure 4.** Excitation of SCN neurons inhibits OVLT-MNC synapses. (a), diagram illustrating the experimental arrangement (see online Methods and Supplementary Figure 1). (b), traces show averages of 15 consecutive EPSCs evoked in an MNC by electrical stimulation of the OVLT (arrows; 0.1 Hz;  $V_{\text{hold}} = -70$  mV) recorded before (control), during (glutamate on SCN) and after (wash) exciting SCN neurons by local application of glutamate. (c), plot showing the average time course of changes in EPSC amplitude at OVLT-MNC synapses during the excitation of SCN neurons with glutamate (gray bar). Each point shows the mean ( $\pm$  s.e.m.) value obtained from 6 cells (the number obtained from each cell was the average of the EPSC amplitude recorded during 4 consecutive sweeps), expressed as a percent of baseline.

## Figure 5

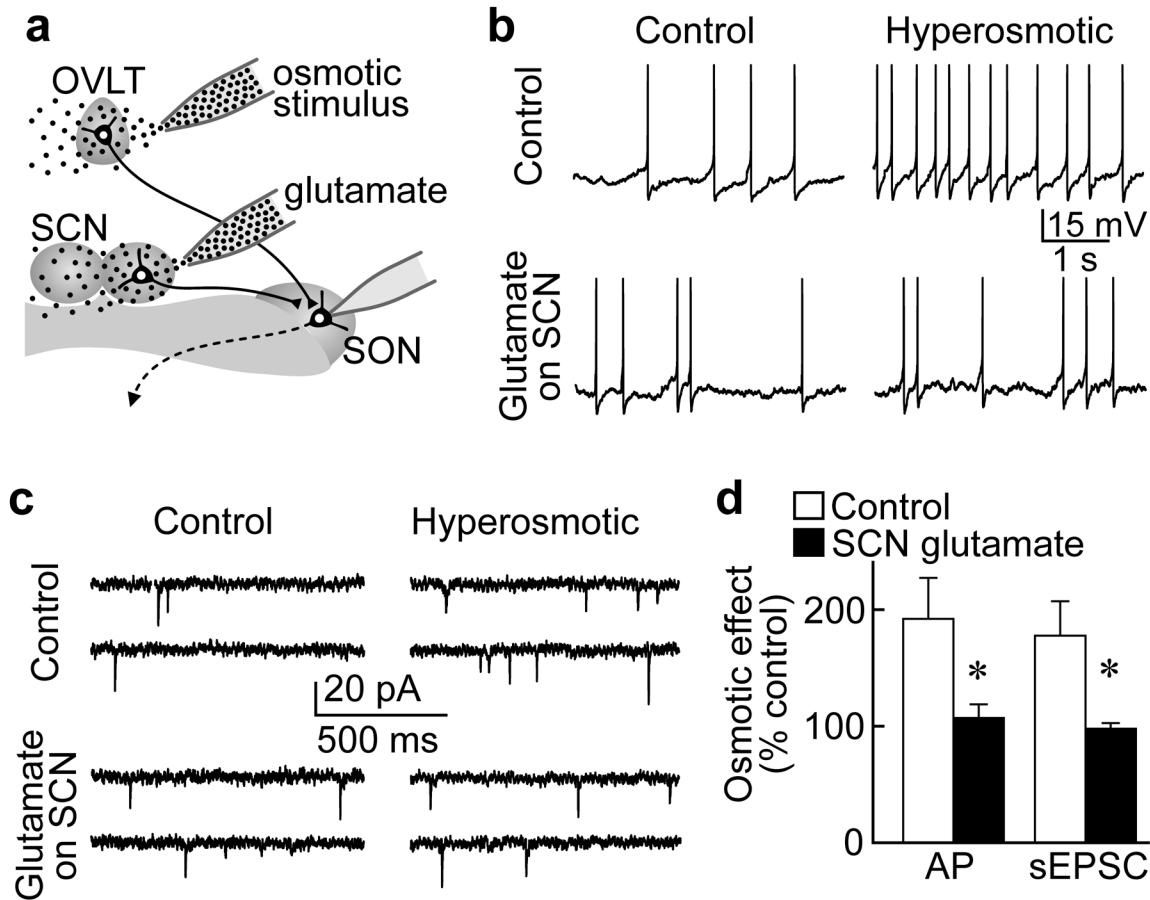


**Figure 5.** Excitation of SCN neurons inhibits activation of MNCs by osmotic stimulation of OVLT. (a), diagram illustrating the experimental arrangement. (b), voltage traces recorded in current clamp show the effects of hyperosmotic stimulation of the OVLT (right panels) on action potential (AP) firing in MNCs compared to control (left panels) when tested either before (upper) or during (lower) local application of glutamate to the SCN. Note the smaller excitatory effect of the osmotic stimulus when glutamate is applied to the SCN. (c), traces (arranged as in b), show examples of sEPSC activity recorded from another MNC under voltage clamp ( $V_{hold} = -70$  mV) during the same protocol as in b. (d), bar graphs show the mean ( $\pm$  s.e.m.) normalized osmotically-induced changes in AP and sEPSC frequency (expressed as percent of baseline) recorded from cells tested before (control) and during the application of glutamate to the SCN. \* indicates  $P < 0.05$ ; paired t-test.

**Figure 6**

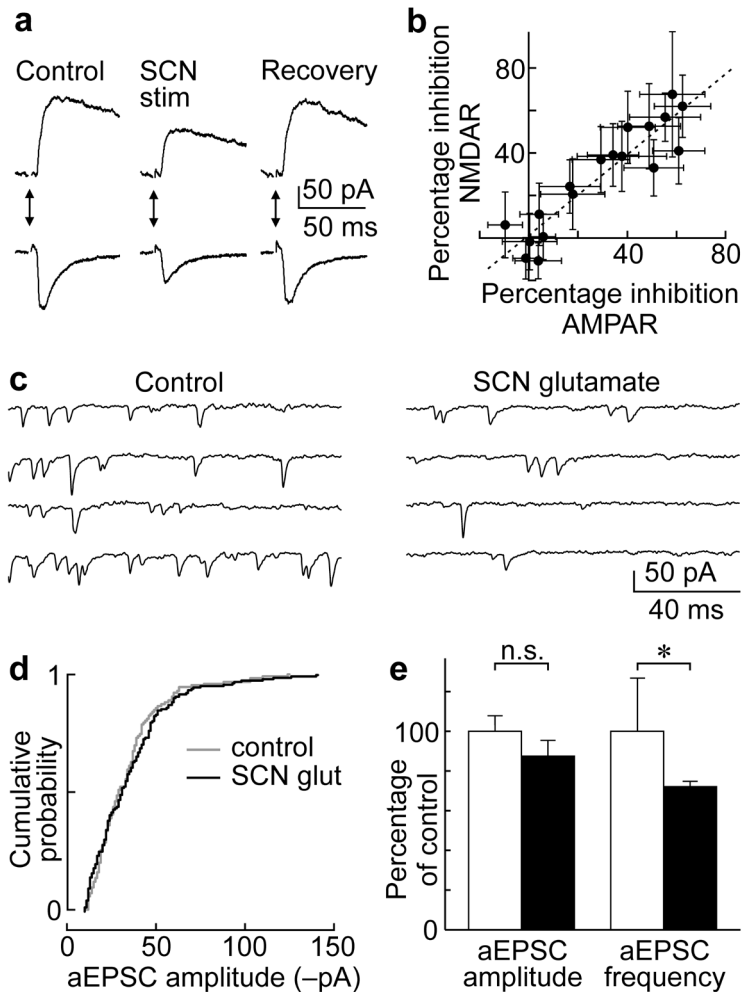


**Figure 6. SCN activation inhibits OVLT-MNC synapses at a presynaptic locus.** (a), examples of OVLT-MNC EPSCs recorded at +40 mV (upper) and -60 mV (lower) before (control) during (SCN stim) and after (recovery) stimulation of the SCN at 5 Hz. Each trace is an average of 15 consecutive sweeps. (b), plot showing the relation between inhibition of the synaptic NMDAR and AMPAR responses during the dynamic (i.e. rising and falling) phases of the SCN effect observed in 8 cells. For each cell the normalized inhibition of the NMDAR (current measured at +40 mV, 75 ms after the OVLT stimulus) and AMPAR (peak current measured at -60 mV) responses were measured during each of 9 sweeps recorded following onset and offset of SCN stimulation (i.e. 18 sweeps in total). The graph plots average ( $\pm$  s.e.m.) values of NMDAR vs AMPAR inhibition during corresponding sweeps. Dashed line is a linear regression fit (slope  $0.96 \pm 0.10$ ;  $r^2 = 0.842$ ;  $n = 18$ ;  $P < 0.0001$ ). (c), examples of aEPSCs recorded during the 200 ms following EPSCs (not shown) evoked before (control) and during excitation of SCN neurons by local application of glutamate. (d), cumulative probability distribution of aEPSC amplitudes (same cell as in c) during control and SCN glutamate. (e), bar graphs plot mean normalized ( $\pm$  s.e.m.) changes in aEPSC amplitude and frequency during SCN stimulation with glutamate. Data are expressed as percent of control, \* indicates  $P < 0.05$ ; n.s. indicates difference not statistically significant.

**Figure 7**

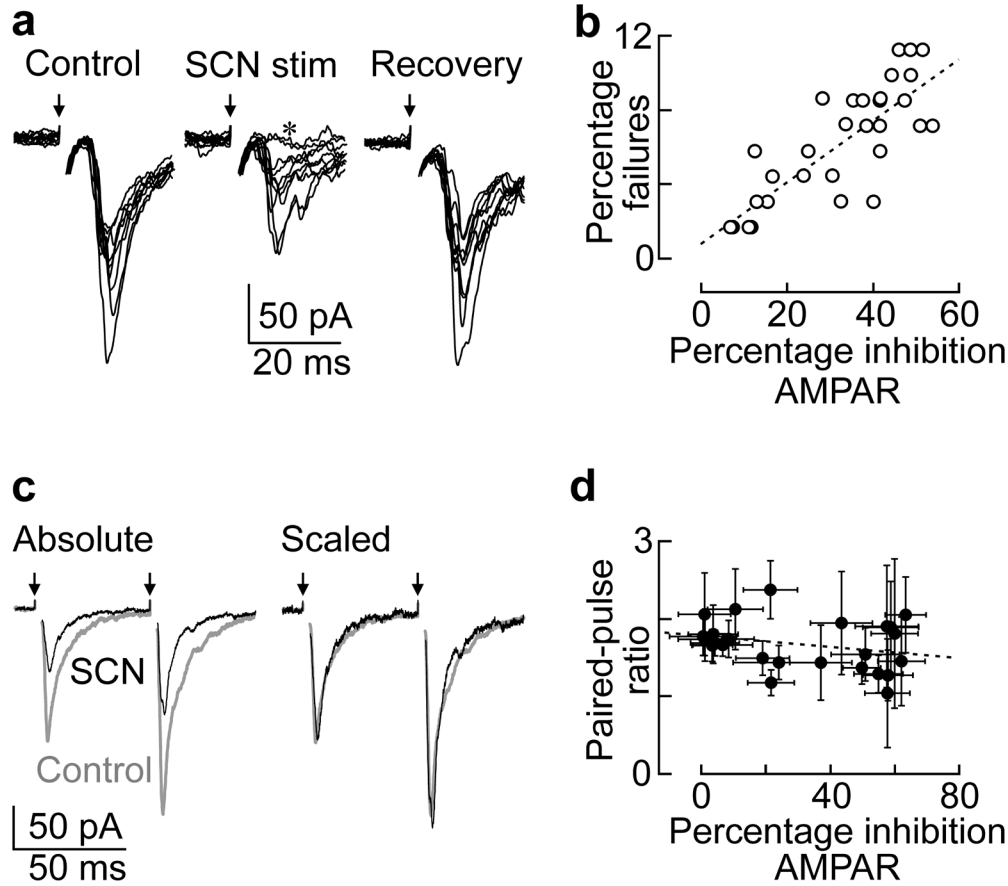


**Figure 7. Effects of SCN stimulation on synaptic failures and frequency-facilitation.** (a), each panel superimposes 10 consecutive sweeps recorded in an MNC with electrical stimulation of the OVLT (arrows) before (control), during (SCN stim) and after (recovery) repetitive SCN stimulation (5 Hz). Note synaptic failures (\*) during SCN stim. (b), plot showing the percentage of cells ( $n = 63$ ) showing failures during each of 15 sweeps recorded after onset and offset (30 sweeps in total) of SCN stimulation at 5 Hz. Each point is plotted as a function of the average inhibition of the AMPAR responses during corresponding sweeps. Dashed line is a regression fit (slope 0.166 ;  $r^2 = 0.645$ ). (c), EPSCs evoked by 2 stimuli delivered to the OVLT 50 ms apart (arrows). Traces are averages of 15 consecutive sweeps taken before (control, gray traces) or during SCN stimulation at 5 Hz (SCN; black traces). Left panel shows superimposed traces at absolute amplitudes. Panel at right shows the same traces scaled to the amplitude of the first EPSC. (d), plot expressing mean ( $\pm$  s.e.m.) values of PPR as a function of the % inhibition of AMPAR responses ( $n = 25$  cells) computed from single sweeps recorded at corresponding time points during 2.5 min periods following the onset and offset of SCN stimulation. Dashed line is a linear regression through the data (slope  $-0.004 \pm 0.003$  ; not significantly different from zero;  $P = 0.192$ ).

**Figure 8**

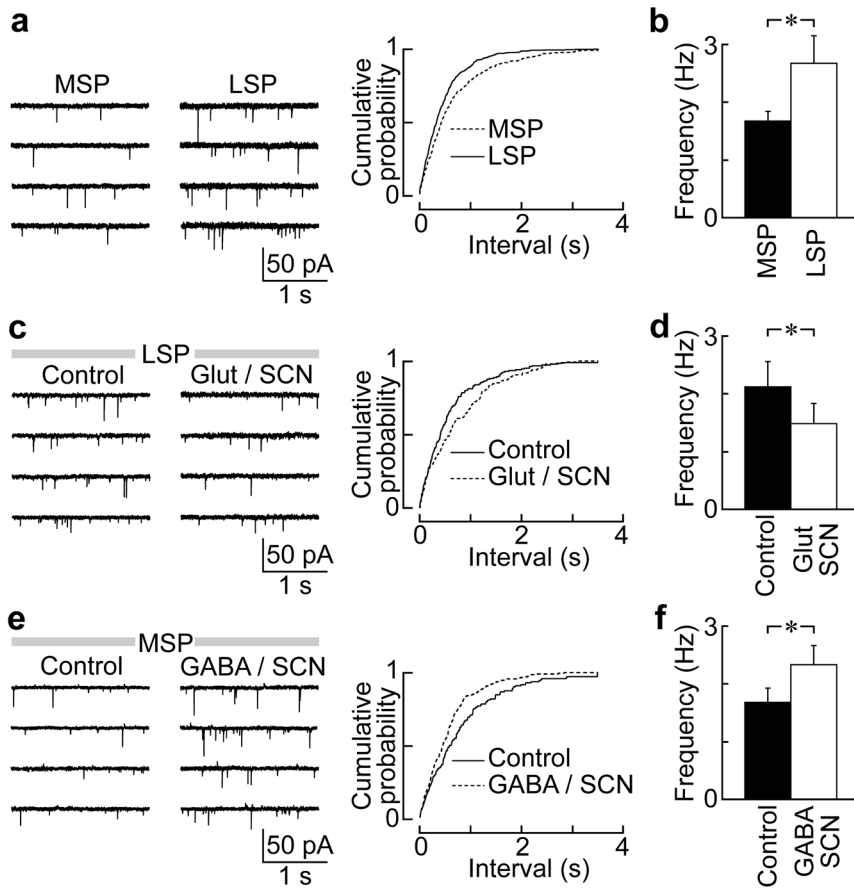


**Figure 8. SCN neurons modulate sEPSC frequency in MNCs.** (a), left panels show examples of sEPSC activity during the MSP (left) and LSP (right). Right panel superimposes cumulative probability distributions of inter-event intervals from the MSP (318 events) and LSP (538 events) cells at left. (b), bar graphs show mean ( $\pm$  s.e.m.) sEPSC frequencies recorded during the MSP ( $n = 32$ ) and LSP ( $n = 44$ ; \*  $P < 0.05$ ). (c), left panels show examples of sEPSC activity during the LSP (gray bar), before (control, left) and during application of glutamate to the SCN (glut/SCN, right). Right panel superimposes cumulative probability distributions of inter-event intervals from the same cell in the absence (control) and presence of glutamate on the SCN (glut/SCN). (d), bar graphs show mean ( $\pm$  s.e.m.) sEPSC frequencies recorded before (control) or during SCN glutamate from 12 MNCs tested during the LSP (\* indicates  $P < 0.05$ ). (e), left panels show examples of sEPSC activity recorded from an MNC during the MSP in the absence of bicuculline (gray bar), before (control) and during application of GABA to the SCN (GABA/SCN). Right panel superimposes cumulative probability distributions of inter-event intervals recorded from the same cell in the absence (control) and presence of GABA/SCN. (f), bar graphs show mean ( $\pm$  s.e.m.) sEPSC frequencies recorded before and during GABA/SCN in 7 MNCs tested during the LSP (\* indicates  $P < 0.05$ ).

## Methods

### *Slice preparation.*

Horizontal hypothalamic slices containing the OVLT, SCN and SON (see Supplementary Figure 1) were prepared from 50-100 g male Long Evans rats (Charles River Canada, St-Constant, QC) as described previously<sup>12</sup>, and in accordance with procedures approved by the Animal Care Committee of McGill University. Briefly, unanaesthetised rats were placed in a plastic restrainer cone (Harvard Apparatus Canada, Saint-Laurent, QC) and killed by decapitation using a small rodent guillotine. The brain was rapidly removed and immersed in near freezing (0 to 4°C) oxygenated (95% O<sub>2</sub>; 5% CO<sub>2</sub>) artificial cerebrospinal fluid (ACSF) comprising (in mM): NaCl, 120; KCl, 3; NaH<sub>2</sub>PO<sub>4</sub>, 1.23; MgCl<sub>2</sub>, 1.48; CaCl<sub>2</sub>, 2; NaHCO<sub>3</sub>, 25.95; and D-glucose 10 (all obtained from Sigma Ltd., St- Louis, MO, except NaCl and CaCl<sub>2</sub> which were purchased from Fisher Scientific, Fair Lawn, NJ). A trimmed block of brain was glued cortex down with the rostral pole facing upwards to a mounting block angled ~40° relative to the horizontal plane. The assembly was then placed in a vibratome and a first cut was made to discard the tissue lying anterior and ventral to the optic tracts and most of the optic chiasma. A single 500 µm, slice was then obtained and transferred dorsal side up to a recording chamber where it was perfused with warmed (32 °C) oxygenated ACSF at a rate of 2-3ml/min. Except where indicated in the text, the ACSF perfusing the slice contained 5 µM bicuculline (Tocris Cookson Inc., Ellisville MO) to block GABA type A (GABA<sub>A</sub>) receptors.

### *Electrophysiology.*

Animals were housed in a room with lights on at 7:00 a.m. and lights off at 19:00 p.m. All recordings were made during the projected LSP (16:00-19:00 p.m.) or MSP (10:00-14:00

a.m.). In each case, slices were prepared about 1 hour prior to the recording session (i.e. ~ 9:00 a.m. for MSP and ~ 15:00 p.m. for LSP). Whole cell recordings from MNCs in the SON were made using patch pipettes prepared from glass capillary tubes (1.2 mm o.d., A-M Systems Inc., Sequim, WA) filled with a solution containing 140 mM potassium gluconate, 2 mM MgCl<sub>2</sub>, 10 mM HEPES, 2 mM di-sodium ATP and 0.4 mM sodium GTP (pH adjusted to 7.25 with NaOH). Pipette resistance in the bath was 2–4 MΩ. Cells were observed on a black and white monitor (Hitachi Denshi Ltd, Japan) using an Olympus BX51WI upright microscope equipped with infrared Differential Interference Contrast optics coupled to a video camera (KP-M1A, Hitachi Denshi Ltd, Japan). Electrodes were visually guided to the cell using a motorized micromanipulator (SD Instruments Inc., Grants Pass, OR) and whole cell recordings were made using an Axopatch-1D amplifier (Molecular Devices Corp., Union City CA). Series resistance was 15–30 MΩ. Membrane current and voltage (d.c.– 2 kHz) was digitized at 5–20 kHz via a digidata 1200B interface coupled to a personal computer running Clampex 8.2 software (Molecular Devices Corp.), which also controlled the timing of electrical stimuli. In experiments where AMPAR and NMDAR currents were respectively monitored at –60 and +40 mV, the solution filling the recording pipette was modified to block Na<sup>+</sup> and K<sup>+</sup> channels, and comprised; 130 mM CsCl, 10 mM NaCl, 10 mM HEPES, 1 mM EGTA, 5 mM QX-314, 2 mM Na<sub>2</sub>ATP and 0.4 mM NaGTP (pH adjusted to 7.2). Single unit extracellular recordings were made using fine-tipped glass pipettes filled with 1.5 M potassium acetate (20–30 MΩ). Pipette voltage was recorded in current-clamp mode with high gain (100X) and the signal was band-pass filtered (500–1500 Hz) using the Clampex software. In whole cell current clamp experiments, the holding current was adjusted to achieve a membrane potential ~ 5 mV below action potential threshold and the cell was allowed to stabilize for > 30 s before testing.

*Electrical, osmotic or chemical stimulation.*

Bipolar stimulating electrodes made from Teflon-coated platinum-iridium wires (60  $\mu\text{m}$  o.d.; A-M Systems Inc., Everett, WA) were placed in the OVLT or SCN as required. Electrical pulses (10 to 70  $\mu\text{A}$ ; 0.1 to 0.5 ms) were delivered via an isolated stimulator (DS2; Digitimer Ltd., Hertfordshire, England) triggered via the acquisition system or a programmable digital timer (D4030; Digitimer Ltd.). Electrical stimulation experiments performed on a large number of slices (> 200) revealed that functional OVLT-SON and SCN-SON synapses are retained in about 75 % of the slices. The effects of electrical stimulation were thus restricted to cells in which EPSCs could be successfully evoked in SON MNCs from both the OVLT and the SON. Where indicated, solutions containing glutamate (25  $\mu\text{M}$ ), GABA (0.5 mM), AMPA (25  $\mu\text{M}$ ) or mannitol (55 mM), all obtained from Sigma Ltd., were dissolved in ACSF and delivered to specific nuclei via a patch pipette connected to a Multi-Channel Picospritzer (General Valve Corp., Fairfield NJ). The osmotic stimulus was delivered by local delivery of a very small volume (< 50  $\mu\text{l}$ ) of mildly concentrated solution (+50 mosmol/kg) injected locally in the parenchyma of the OVLT using a glass pipette with a tip diameter of about 10  $\mu\text{m}$ . The direction of ACSF flow over the slice (see Supplementary Figure 1c) was adjusted to avoid effects of solutions puffed in one nucleus on other nuclei. Moreover, control experiments using extracellular recordings on large numbers of neurons at various positions relative to the tip of a puffing pipette delivering either glutamate or GABA confirmed that lateral diffusion was not a significant factor beyond a radius of 200  $\mu\text{m}$  from the site of injection (not shown). When puffing solutions onto a specific nucleus we could not first establish if functional connections of interest were retained (i.e. by using direct electrical stimulation of the targeted region). Therefore in these cases the analysis was restricted to those cells in which a positive effect of local delivery could be established under control conditions. Specifically, the analysis of

experiments involving the delivery of glutamate over the SCN were limited to cells in which the glutamate stimulus was observed to reduce (by  $\geq 5\%$ ) the basal frequency of APs or sEPSCs. Similarly, the analysis of experiments involving hypertonic stimulation of the OVLT was restricted to SON MNCs in which the stimulus was able to induce a detectable ( $\geq 5\%$ ) increase in the frequency of APs or sEPSCs in control conditions.

#### *Data analysis.*

All recordings were analyzed using Clampfit 9.0 (Molecular Devices Corp.). Action potentials and sEPSCs were detected automatically using the event detection routine of the software. To quantify changes in sEPSC and/or action potential frequency during local chemical stimulation of the SCN (Figures 5 and 8) and/or osmotic stimulation of the OVLT (Figures 1 and 5), average frequency measured 60 s before the onset of the stimulus (i.e. baseline) was compared to the peak average frequency observed during a 30 s segment of the data recorded while the stimulus was being applied. Detection and measurement of individual aEPSCs was done manually using Clampfit 9. Cumulative probability plots were constructed using Clampfit. The curve shown in Fig. 3c was fitted to the data using Sigmaplot 8.0 (SPSS Inc, Chicago IL) applying a three parameter Logistic equation ( $y = a / [1/(1 + x/x_0)^b]$ ), where  $a$  is the maximum amplitude of the effect,  $b$  is a slope factor and  $x_0$  is the frequency at half amplitude.

#### *Statistical Analysis.*

All values in this study are reported as mean  $\pm$  standard error of the mean ( $\pm$  s.e.m.).

Linear regressions through the data were performed using Sigmaplot. Comparisons between two

means were performed using Student's paired or unpaired t-test, as appropriate. To establish the presence or absence of a significant correlation, the slope of a linear regression was compared to a slope of 0 (no correlation) using Prism 4.0 (GraphPad Software, Inc. San Diego CA, USA). In all statistical comparisons, differences were considered significant when  $P < 0.05$ .

## References

1. Bicknell, R.J. Optimizing release from peptide hormone secretory nerve terminals. *J Exp Biol* **139**, 51-65 (1988).
2. Bourque, C.W. Central mechanisms of osmosensation and systemic osmoregulation. *Nat Rev Neurosci* **9**, 519-531 (2008).
3. Robertson, G.L., Shelton, R.L. & Athar, S. The osmoregulation of vasopressin. *Kidney Int* **10**, 25-37 (1976).
4. Forsling, M.L. Diurnal rhythms in neurohypophysial function. *Exp Physiol* **85 Spec No**, 179S-186S (2000).
5. Miller, M. Nocturnal polyuria in older people: pathophysiology and clinical implications. *J Am Geriatr Soc* **48**, 1321-1329 (2000).
6. Granda, T.G., Velasco, A. & Rausch, A. Variations and interrelation between vasopressin and plasma osmolality in diabetic rats with insulin treatment. *Life Sci* **63**, 1305-1313 (1998).
7. Gordon, C.R. & Lavie, P. Day-night variations in urine excretions and hormones in dogs: role of autonomic innervation. *Physiol Behav* **35**, 175-181 (1985).
8. Claybaugh, J.R., Sato, A.K., Crosswhite, L.K. & Hassell, L.H. Effects of time of day, gender, and menstrual cycle phase on the human response to a water load. *Am J Physiol Regul Integr Comp Physiol* **279**, R966-973 (2000).
9. Richard, D. & Bourque, C.W. Synaptic control of rat supraoptic neurones during osmotic stimulation of the organum vasculosum lamina terminalis in vitro. *J Physiol* **489** ( Pt 2), 567-577 (1995).

10. Ciura, S. & Bourque, C.W. Transient receptor potential vanilloid 1 is required for intrinsic osmoreception in organum vasculosum lamina terminalis neurons and for normal thirst responses to systemic hyperosmolality. *J Neurosci* **26**, 9069-9075 (2006).
11. Vivas, L., Chiaraviglio, E. & Carrer, H.F. Rat organum vasculosum laminae terminalis in vitro: responses to changes in sodium concentration. *Brain Res* **519**, 294-300 (1990).
12. Trudel, E. & Bourque, C.W. A rat brain slice preserving synaptic connections between neurons of the suprachiasmatic nucleus, organum vasculosum lamina terminalis and supraoptic nucleus. *J Neurosci Methods* **128**, 67-77 (2003).
13. Maywood, E.S., O'Neill, J.S., Chesham, J.E. & Hastings, M.H. Minireview: The circadian clockwork of the suprachiasmatic nuclei--analysis of a cellular oscillator that drives endocrine rhythms. *Endocrinology* **148**, 5624-5634 (2007).
14. Reppert, S.M. & Weaver, D.R. Coordination of circadian timing in mammals. *Nature* **418**, 935-941 (2002).
15. Brown, T.M. & Piggins, H.D. Electrophysiology of the suprachiasmatic circadian clock. *Prog Neurobiol* **82**, 229-255 (2007).
16. Kent, J. & Meredith, A.L. BK channels regulate spontaneous action potential rhythmicity in the suprachiasmatic nucleus. *PLoS ONE* **3**, e3884 (2008).
17. Hallworth, R., Cato, M., Colbert, C. & Rea, M.A. Presynaptic adenosine A1 receptors regulate retinohypothalamic neurotransmission in the hamster suprachiasmatic nucleus. *J Neurobiol* **52**, 230-240 (2002).
18. Kalsbeek, A. & Buijs, R.M. Output pathways of the mammalian suprachiasmatic nucleus: coding circadian time by transmitter selection and specific targeting. *Cell Tissue Res* **309**, 109-118 (2002).
19. van den Pol, A.N. Glutamate and GABA presence and action in the suprachiasmatic nucleus. *J Biol Rhythms* **8 Suppl**, S11-15 (1993).
20. Oliet, S.H. & Poulain, D.A. Adenosine-induced presynaptic inhibition of IPSCs and EPSCs in rat hypothalamic supraoptic nucleus neurones. *J Physiol* **520 Pt 3**, 815-825 (1999).

21. Kombian, S.B., Zidichouski, J.A. & Pittman, Q.J. GABAB receptors presynaptically modulate excitatory synaptic transmission in the rat supraoptic nucleus in vitro. *J Neurophysiol* **76**, 1166-1179 (1996).
22. Schrader, L.A. & Tasker, J.G. Presynaptic modulation by metabotropic glutamate receptors of excitatory and inhibitory synaptic inputs to hypothalamic magnocellular neurons. *J Neurophysiol* **77**, 527-536 (1997).
23. Hirasawa, M., Mougnot, D., Kozoriz, M.G., Kombian, S.B. & Pittman, Q.J. Vasopressin differentially modulates non-NMDA receptors in vasopressin and oxytocin neurons in the supraoptic nucleus. *J Neurosci* **23**, 4270-4277 (2003).
24. Derkach, V.A., Oh, M.C., Guire, E.S. & Soderling, T.R. Regulatory mechanisms of AMPA receptors in synaptic plasticity. *Nat Rev Neurosci* **8**, 101-113 (2007).
25. Citri, A. & Malenka, R.C. Synaptic plasticity: multiple forms, functions, and mechanisms. *Neuropsychopharmacology* **33**, 18-41 (2008).
26. Iremonger, K.J. & Bains, J.S. Integration of asynchronously released quanta prolongs the postsynaptic spike window. *J Neurosci* **27**, 6684-6691 (2007).
27. Zucker, R.S. Short-term synaptic plasticity. *Annu Rev Neurosci* **12**, 13-31 (1989).
28. Raiteri, M. Presynaptic metabotropic glutamate and GABAB receptors. *Handb Exp Pharmacol*, 373-407 (2008).
29. Kolaj, M., Yang, C.R. & Renaud, L.P. Presynaptic GABA(B) receptors modulate organum vasculosum lamina terminalis-evoked postsynaptic currents in rat hypothalamic supraoptic neurons. *Neuroscience* **98**, 129-133 (2000).
30. Inouye, S.T. & Kawamura, H. Persistence of circadian rhythmicity in a mammalian hypothalamic "island" containing the suprachiasmatic nucleus. *Proc Natl Acad Sci U S A* **76**, 5962-5966 (1979).
31. Shibata, S., Oomura, Y., Kita, H. & Hattori, K. Circadian rhythmic changes of neuronal activity in the suprachiasmatic nucleus of the rat hypothalamic slice. *Brain Res* **247**, 154-158 (1982).
32. Green, D.J. & Gillette, R. Circadian rhythm of firing rate recorded from single cells in the rat suprachiasmatic brain slice. *Brain Res* **245**, 198-200 (1982).

33. Groos, G. & Hendriks, J. Circadian rhythms in electrical discharge of rat suprachiasmatic neurones recorded in vitro. *Neurosci Lett* **34**, 283-288 (1982).
34. Herzog, E.D., Takahashi, J.S. & Block, G.D. Clock controls circadian period in isolated suprachiasmatic nucleus neurons. *Nat Neurosci* **1**, 708-713 (1998).
35. Brimble, M.J. & Dyball, R.E. Characterization of the responses of oxytocin- and vasopressin-secreting neurones in the supraoptic nucleus to osmotic stimulation. *J Physiol* **271**, 253-271 (1977).
36. Brimble, M.J., Dyball, R.E. & Forsling, M.L. Oxytocin release following osmotic activation of oxytocin neurones in the paraventricular and supraoptic nuclei. *J Physiol* **278**, 69-78 (1978).
37. Huang, W., Lee, S.L. & Sjoquist, M. Natriuretic role of endogenous oxytocin in male rats infused with hypertonic NaCl. *Am J Physiol* **268**, R634-640 (1995).
38. Huang, W., Lee, S.L., Arnason, S.S. & Sjoquist, M. Dehydration natriuresis in male rats is mediated by oxytocin. *Am J Physiol* **270**, R427-433 (1996).
39. Verbalis, J.G., Mangione, M.P. & Stricker, E.M. Oxytocin produces natriuresis in rats at physiological plasma concentrations. *Endocrinology* **128**, 1317-1322 (1991).
40. Kalsbeek, A., *et al.* Minireview: Circadian control of metabolism by the suprachiasmatic nuclei. *Endocrinology* **148**, 5635-5639 (2007).
41. Honda, K., Negoro, H., Higuchi, T. & Tadokoro, Y. The role of the anteroventral 3rd ventricle area in the osmotic control of paraventricular neurosecretory cells. *Exp Brain Res* **76**, 497-502 (1989).
42. Leng, G., Blackburn, R.E., Dyball, R.E., Russell, J.A. Role of anterior peri-third ventricular structures in the regulation of supraoptic neuronal activity and neurohypophysial hormone secretion in the rat. *Journal of Neuroendocrinology* **1**, 35-46 (1989).
43. Buijs, R.M. Intra- and extrahypothalamic vasopressin and oxytocin pathways in the rat. Pathways to the limbic system, medulla oblongata and spinal cord. *Cell Tissue Res* **192**, 423-435 (1978).

44. Kombian, S.B., Mougnot, D. & Pittman, Q.J. Dendritically released peptides act as retrograde modulators of afferent excitation in the supraoptic nucleus in vitro. *Neuron* **19**, 903-912 (1997).
45. Kombian, S.B., Mougnot, D., Hirasawa, M. & Pittman, Q.J. Vasopressin preferentially depresses excitatory over inhibitory synaptic transmission in the rat supraoptic nucleus in vitro. *J Neuroendocrinol* **12**, 361-367 (2000).
46. Bamford, N.S., *et al.* Repeated exposure to methamphetamine causes long-lasting presynaptic corticostriatal depression that is renormalized with drug readministration. *Neuron* **58**, 89-103 (2008).
47. Delaney, A.J., Crane, J.W. & Sah, P. Noradrenaline modulates transmission at a central synapse by a presynaptic mechanism. *Neuron* **56**, 880-892 (2007).
48. Panatier, A., Gentles, S.J., Bourque, C.W. & Oliet, S.H. Activity-dependent synaptic plasticity in the supraoptic nucleus of the rat hypothalamus. *J Physiol* **573**, 711-721 (2006).
49. Panatier, A., *et al.* Glia-derived D-serine controls NMDA receptor activity and synaptic memory. *Cell* **125**, 775-784 (2006).
50. Tully, K., Li, Y. & Bolshakov, V.Y. Keeping in check painful synapses in central amygdala. *Neuron* **56**, 757-759 (2007).